

INFLUENCE OF DISLOCATIONS ON BUMPS OCCURRENCE IN DEEP MINES

Petr Pavel PROCHÁZKA ^{1)*}, Jiřina TRČKOVÁ ²⁾ and Tat Seng LOK ³⁾

¹⁾ Association of Czech Engineers, Komornická, 130 00 Prague, Czech Republic

²⁾ Institute of Rock, Structure and Mechanics, Czech Academy of Science of the Czech Republic, v.v.i.,
V Holešovičkách 41, 182 09 Prague, Czech Republic

³⁾ School of Civil and Environmental Engineering, Nanyang Technological University, 639798 Singapore

*Corresponding author's e-mail: petr.proch@volny.cz

(Received October 2010, accepted November 2010)

ABSTRACT

The problem of bumps occurrence in deep mines during the long wall mining appears to be one of the most serious one in the design of engineering of mining. The bumps are caused for various reasons, but basically it is an aftermath of the accumulated energy, which is released under some unfavorable conditions. In this paper the influence of given dislocations and their slope in a coal seam are studied based. The numerical tool is the free hexagon method. This method belongs to a set of discrete element methods and enables us to define and calculate stresses in a natural way along the interfacial boundaries of adjacent particles (elements). Since the bumps are affected by a possible slip along the dislocations, dynamical response has to be taken into account. The velocity of excavation of the mine is considered by successive change of values of Eshelby's forces on the face of the wall.

KEYWORDS: numerical modeling, free hexagon method, deep mines, bumps occurrence

1. INTRODUCTION

In deep mines the problem of bumps occurrence during the long wall mining belongs to one of the most serious one from the set of problems to be solved in the project stage of mining engineering. It causes disaster of such an extent that human lives are lost, material and energy expenses are enormous and renovation of the afflicted mine is almost impossible. The reason for bumps occurrence consists in accumulation of extremely great energy in the neighborhood of the mine face and its release under certain conditions. In former papers of the first author, e.g. (Procházka, 2004), the triggering conditions have been exclusively based on an assumption of nucleation of cracks in front of the mine face (side walls). In the above said paper the formulation and solution was presented as stability problem and only statical conditions had to be fulfilled. Considering a possible slip along the dislocation due to human activities also the inertia terms play an important role and have to be embodied in the formulation. In the approximate formulation their appearance desires a special treatment. This approach basically follows the well-known ideas of PFC (particle flow code), (Cundall, 1971) and (Cundall et al., 1979). Certain theoretical background of the PFC can be found in (Moreau, 1994). On the other hand, a disadvantage of

the PFC consists in the fact that a possible bond of the particles is realized at points of the contact boundary of adjacent particles, so that the calculation of stresses is quite inaccurate. This fault is removed in the present theory and the numerical approach.

(Wei et al., 2009) published new approaches in geodynamics of rock linked with the bumps occurrence in a continuous model.

It is well known that there are not too many papers on rock bursts in the literature. It is worth noting some other methods, which start with a continuous formulation, but can simulate possible splitting of rock parts. Among such the Manifold method belongs, (Ma et al., 2010).

A slip along a dislocation can be solved in a very natural way using dynamical version of Uzawa's algorithm, (Procházka and Sejnoha, 1995), for example. By virtue of separation of domains being defined on both sides of the dislocation even linear equations can characterize the behavior of the underground continuum. The only problem occurs on how to describe the behavior (possibly nonlinear) in the separated parts of the underground continuum.

The mechanical properties and other data being necessary for correct computation have been first consulted with experiments published by (Haramy et al., 1995), and in (Procházka and Vacek, 2002) scale

models were prepared for simulating bumps in laboratory. Couple of experimental studies has been carried out on scale models describing this phenomenon in real mines in Bohemia. The experiments make more viewable phenomena, such as the overall properties, failure strength of the material, surface cracking, and others, which can be seen from outside of the sample tested. Using high speed video camera other detailed information about important properties of reason and development of the bumps was obtained. A comparison of the calculated and observed results from experiments is partly published in (Procházka, 2004).

In the method put forward in this paper the domain describing both the rock and coal seams is divided into hexagonal elements (particles) of an arbitrary shape, which are mutually disjoint and non-overlapping. The material of each hexagon behaves linearly, i.e. linear Hooke's law is assumed, as small enough particles are considered. The only nonlinearities are moved to the interfacial boundaries between adjacent elements. The interfaces obey the generalized Mohr-Coulomb hypotheses, (Procházka and Sejnoha, 1995), for example, and the material is identified by the parameters, which are well known from soil or rock mechanics. Among those parameters the angle of internal friction, cohesion (shear strength), tensile strength, and others belong to the input data for the computation. Naturally, the behavior inside of the elements can also be regarded as nonlinear, but if small enough elements are presumed, this assumption is superfluous.

Since the cracking in the rock mass is not a priori known, the fracture mechanics problem turns to contact problem in this paper. Moreover, the Uzawa's algorithm can be properly applied if not too many cracks are anticipated. This is obviously not true in this case and the penalty formulation is postulated in the method of free hexagons. The mechanical explanation of the penalty method is very easy, as the penalties are represented by spring stiffnesses. As the radial (tension or compression) and tangential (shear) constrain between adjacent elements exist, both radial and shear springs have to be reflected.

The situation inside of each particle is described by boundary elements, (Brebbia et al., 1984), for example, which can involve also inertia terms. This advantage is not utilized in the presented approach; the formulation in particles is based on static equilibrium. The inertia terms are, similarly to the PFC, lumped at the centers of the particles. The stencil for the description of the time development starts with finite difference scheme, and is basically identical with the PFC model, but the hierarchy of computation of the time derivatives – D'Alembert forces, acceleration, velocity and displacements – is ordered conversely.

The time dependent excavation of the underground opening is described by Eshelby's forces, (Eshelby, 1963). They are applied to the wall

of the opening and their time dependent (successive) increase characterizes the velocity of mining. Similar approach is used when describing an opening of tunnel with lining, digging a ditch and also, which is the original application of the Eshelby description of the influence of the change of temperature in fibers in the theory of composites.

The free hexagon method was successfully applied to coupled modeling in underground structures, (Procházka and Trčková, 2008), where only static case was exploited.

In this paper a special problem of the assessment of bumps occurrence in deep mines is discussed. It is dealt with a mutual interaction of predisposed dislocations filled by gas in coal seams. More precisely, the effect of slopes of the dislocations is studied and the approach on how to proceed if the gas appears in the dislocations. Based on the method of free hexagons viewable post-processing enables the consultant to decide in future steps of mining.

First the philosophy of the case considered is explained and the basic idea of the method of free hexagons is put forward. For the description of behavior inside of one particle (element) boundary element method is used, which is briefly presented in the next section. Then the contact conditions expressed by a soft contact (using spring stiffness) between adjacent particles and Fischera's conditions are discussed. Since the particles accelerate essentially, inertia forces are taken into consideration, too. Transformation of spring stiffness is derived in what follows and typical examples conclude the paper, showing the ability of the theory.

2. BASIC ASSUMPTIONS

In order to explain the basic phenomenon of bumps consider the structure of a coal seam and surrounding rock as demonstrated in Figure 1. In the virgin state the stresses are uniformly distributed along the interface of the coal seam and the overburden. After the adit is excavated the redistribution of those stresses causes that the load of the side faces (walls) of the opening increases principally. Moreover, in many cases the coal seam is cracked and the cracks are filled by gas, which is pull out due to the increase of the pressure at the contact among the overburden, coal and adit; this circumstance raises the danger of instability. Two important problems are of basic interest to us:

- the velocity of excavation (the faster the excavation, the greater danger of bumps occurrence)
- the slope of cracks in the seam.

Since there is no general intimacy about the way of loss of stability due to a damage behavior of both the rock and overburden, each option of movement should basically be taken into account. This is why discrete element methods (DEM) have been established.

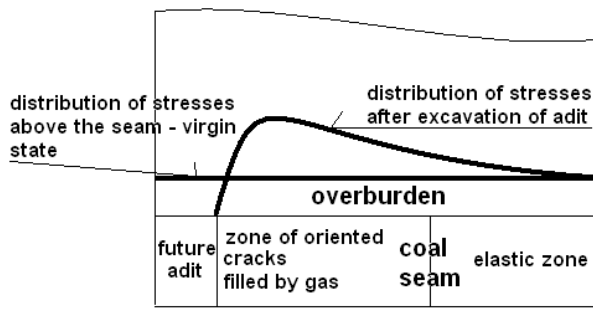


Fig. 1 Description of properties of a coal seam and distribution of vertical stresses at different stages.

Under the assumption that the material properties of both rock and coal are known, hexagon elements are created and linear behavior in them is supposed. Since the elements are considered to be small enough, isotropic and homogeneous case is taken into account, i.e. the elements are homogeneous and isotropic with material characterizations given by modulus of elasticity E and Poisson's ratio ν , for example.

Classical problem involving generalized Coulomb's law together with the exclusion of tensile stress exceeding the tensile strength along the interfaces (possible dislocations) is solved instead of using approaches given by the fracture mechanics. The reason of such a formulation consists in the fact that the material properties are identified in a much better way than in the case different from the formulation in terms of a contact problem.

A typical set up of adjacent elements is illustrated in Figure 2. In what follows the uniformly distributed mass density inside of each element is substituted by concentration of it at the center of gravity of the elements. Then first the solution of elastic problem in an element is formulated and after this the element is put into neighborhood of adjacent elements. The current element is put into a neighborhood of the other elements, which are for a moment frozen. The statical equilibrium in the current element is fulfilled with the inertia forces lumped into the center of gravity of the elements, as well. The current element moves according some prescribed rule through all possible locations in the domain describing the system coal – overburden. This is carried out at each time interval. By such an iteration the final state is achieved and either no significant movements are attained or too extensive displacements occur. In the second case the bumps is probable. This is also the case when the iterative process diverges.

Regular distribution of elements is assumed, i.e. only one matrix relating tractions and boundary displacements is a priori prepared. Also 2D problem is solved as fully sufficient for describing the threat of bumps in deep mines.

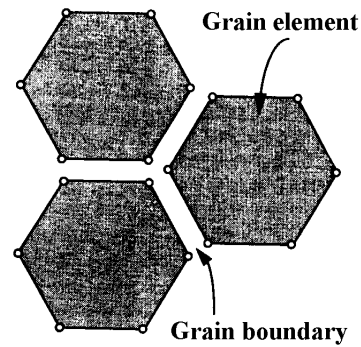


Fig. 2 Adjacent grains set up.

3. BOUNDARY ELEMENT SOLUTION IN ONE ELEMENT

A typical element in undeformed state is described by the domain Ω and the boundary is Γ . As said before, two-dimensional case is considered as fully representative. The elastic distribution of displacements, strains and stresses is described by the boundary element method. The solution of elasticity on each hexagonal element is approximated by concentration of DOFs at the centers of boundary abscissas of the hexagonal element under consideration, and the distribution of both the boundary displacements and tractions along the edges of this hexagon are assumed to be uniform. Note that higher order approximation can be used. For example, if a linear distribution of both the tractions and displacements is supposed, the approximation seems to be better. This is not quite true. Obviously, the mechanical behavior inside of the particles is characterized probably better, but in the complete system some disturbances can occur, which are different from reality, as too rigid form of particles is not wanted. If even quadratic or cubic approximation is introduced, curvilinear hexagons are attained. Then the prescription of the interfacial condition is almost impossible. Here similar rule as in the linear approximation holds valid: The higher approximation can harm the numerical results and complicates the numerical computation very much. For small elements, which are required in every case, the higher approximation in the sense of boundary elements do not bring about any benefit.

Then, generally, the integral equations formulate the problem on a selected particle:

$$c_{ik}u_k(\xi) = \int_{\Gamma} p_i(\mathbf{x})u_{ik}^*(\mathbf{x},\xi)d\mathbf{x} - \int_{\Gamma} u_i(\mathbf{x})p_{ik}^*(\mathbf{x},\xi)d\mathbf{x} + \int_{\Omega} b_i(\mathbf{x})u_{ik}^*(\mathbf{x},\xi)d\mathbf{x} \quad (1)$$

where i and k run 1, 2, and $s = 1, \dots, 6$, δ_{ij} is the Kronecker delta. Fields $\mathbf{u} = \{u_1, u_2\}$ and $\mathbf{p} = \{p_1, p_2\}$ denote displacements and tractions, respectively. Point $\mathbf{x} = \{x_1, x_2\}$ is the integration point and

$\xi = \{\xi_1, \xi_2\}$ is the observer. The terms with asterisk are known kernels, the fundamental solutions of the problem of 2D elasticity, which arise from the solution of source problem in unbounded area.

In case the regular hexagons are used and a uniform distribution of both displacements and tractions is used, the situation is very easy from the standpoint of calculation. Although point-wise contact is then assumed the stresses are determined at a high accuracy. Moreover, the shape of the particles is not restricted as in the case of linear distribution of variables along the interfacial boundaries. In case the uniform approximation is applied, $c_{ik} = \frac{1}{2} \delta_{ik}$ and then

$$\frac{1}{2} \delta_{ik} u_k(\xi) = \int_{\Gamma} p_i(\mathbf{x}) u_{ik}^*(\mathbf{x}, \xi) d\mathbf{x} - \int_{\Gamma} u_i(\mathbf{x}) p_{ik}^*(\mathbf{x}, \xi) d\mathbf{x} + \int_{\Omega} b_i(\mathbf{x}) u_{ik}^*(\mathbf{x}, \xi) d\mathbf{x} \quad (2)$$

The quantities with asterisks are given kernels, which for the plain strain state can be listed as, see (Brebbia et al., 1984), for example:

$$u_{ij}^* = \frac{1}{8\pi(1-\nu)G} [(3-4\nu) \log(1/r) \delta_{ij} - \frac{r_i r_j}{r^2}],$$

$$p_{ij}^* = -\frac{1}{4\pi(1-\nu)r} \left\{ \frac{dr}{dn} [(1-2\nu) \delta_{ij} + \frac{2r_i r_j}{r^2}] + (1-2\nu) \left(\frac{r_j}{r} n_i - \frac{r_i}{r} n_j \right) \right\}, \quad (3)$$

$$\sigma_{ij\alpha}^* = -\frac{1}{4\pi(1-\nu)r} \left[(1-2\nu) \left(-\frac{r_i}{r} \delta_{j\alpha} + \frac{r_j}{r} \delta_{i\alpha} + \frac{r_\alpha}{r} \delta_{ij} \right) + \frac{2r_i r_j r_\alpha}{r^3} \right],$$

where ν is Poisson's number, G is the shear modulus, $r_i = x_i - \xi_i$, $r^2 = r_1^2 + r_2^2$, and $\mathbf{n} = \{n_1, n_2\}$ is the unit outward normal.

Knowing the form of kernels and substituting the approximations for boundary displacements and tractions, matrix equations are obtained:

$$\mathbf{A}\mathbf{u} = \mathbf{B}\mathbf{p} + \mathbf{b}, \quad \mathbf{K}\mathbf{u} = \mathbf{p} + \mathbf{V} \quad (4)$$

where \mathbf{A} , \mathbf{B} and \mathbf{K} are square matrices (12 * 12), \mathbf{u} is the vector of displacement approximations at vertices, \mathbf{p} that of tractions and \mathbf{b} and \mathbf{V} are vectors of volume weight influences. The latter are vectors (1*12). Note that the matrix \mathbf{K} plays a role of the stiffness matrix in finite elements, but here is non-symmetric and full (not banded). The transfer from the first relation (4) to the second is enabled by the fact that the matrix \mathbf{B} is regular and therefore can be inverted.

In Figure 3 various shapes of deformed elements are shown. The shape is in accordance with the uniform or linear approximation of the displacements and tractions along the boundary elements, it means

that no deformation of the edges of hexagons can appear. In the second case in the picture the elements can even lose convexity in the deformed state. This case does not make any harm on solvability and uniqueness of the problem.

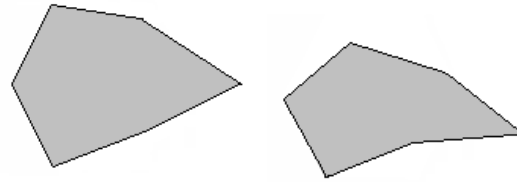


Fig. 3 Deformed shapes of hexagons due to the selected approximation.

4. STATIC CONTACT CONDITIONS

Let us consider hexagon i being in possible contact with neighboring hexagons j_1, \dots, j_6 , see Figure 4. In the next denotation we omit j and identify the neighbors by indices 1, ..., 6. Then in Figure 4 $N_{ik} = N_{ki}$ is the resultant of the traction p_n acting in the normal direction to the interface between elements i and j_k , $T_{ik} = T_{ki}$ is the resultant of the shear traction p_t acting along the interface between elements i and j_k . The indices of N and T must commute as the action – reaction law takes place. In Figure 5 denotation of soft contact modeled by springs in both normal and tangential directions is seen. Symbols k_n and k_t stand for spring stiffnesses in normal and tangential directions, respectively, acting along the appropriate interface.

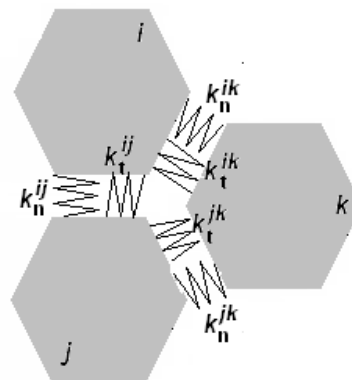


Fig. 4 Denotation and meaning of springs constraining three neighboring elements

5. FISCHERA'S CONDITIONS

Fischera's conditions have been formerly formulated for an admissible set being a cone. This is exactly the case of the normal strength equal to zero. In our case the conditions in normal direction should be rather improved as there is also the tensile strength to be taken into account. Fischera's conditions can be written in this case as:

$$\begin{aligned} p_n^+ \kappa(p_n^+ - p_n) - p_n &\geq 0, [u]_n \geq 0 \\ \{p_n^+ \kappa(p_n^+ - p_n) - p_n\} [u]_n &= 0, \end{aligned} \quad (5)$$

In the tangential direction the particles are also connected by springs, which relate the shear forces and the displacements in tangential direction to the interfacial boundary.

Hence, in the tangential direction it holds:

$$\begin{aligned} c \kappa(p_n^+ - p_n) - p_n \tan \phi - |p_t| &\geq 0, |[u]_t| \geq 0, \\ \{c \kappa(p_n^+ - p_n) - p_n \tan \phi - |p_t|\} [u]_t &= 0 \end{aligned} \quad (5a)$$

In formulas (5) and (5a) $\mathbf{p} = \{p_n, p_t\}$ is the vector of tractions with components projected in normal and tangential directions to the interface, respectively, p_n^+ is the tensile strength, $\kappa(\cdot)$ means the Heaviside function being 1 for positive argument and zero otherwise, $[u]_n, [u]_t$ are jumps in the displacements in normal and tangential directions, respectively. As for the traction no jump is allowed, but action-reaction law has to be fulfilled. It is worth noting that this is not valid in an exceptional construction of tunnels with linings, where Eshelby's forces are exactly the differences between the interfacial tractions appearing along the interface between the lining and surrounding rock. Material constants are the angle of internal friction ϕ and the cohesion (shear strength) c .

The energy of the system can be stored as:

$$\begin{aligned} \Pi &= \frac{1}{2} \sum_{\alpha=1}^N a_\alpha(\mathbf{u}, \mathbf{u}) - \int_\Gamma \bar{\mathbf{p}}^T \mathbf{u} \, dx - \\ &- \sum_{\beta=1}^n \int_{\Gamma_\beta} \{(p_n^+)^{\beta} \kappa(p_n^+ - p_n^{\beta}) - p_n^{\beta}\} [u]_n^{\beta} \, dx - \\ &- \sum_{\beta=1}^n \int_{\Gamma_\beta} \{c^{\beta} \kappa(p_n^+ - p_n^{\beta}) - p_n^{\beta} \tan \phi - |p_t^{\beta}|\} |[u]_t^{\beta}| \, dx \end{aligned} \quad (6)$$

where α runs over all hexagon elements, $\alpha = 1, \dots, N$, β runs over all contact edges of possible contacts Γ_β , $\beta = 1, \dots, n$, Γ is the external boundary where \mathbf{p} is prescribed, and

$$a_\alpha(\mathbf{u}, \mathbf{u}) = \int_{\Omega_\alpha} (\boldsymbol{\sigma}^\alpha)^T \boldsymbol{\varepsilon}^\alpha \, dx \quad (7)$$

is the internal energy (bilinear form) inside a hexagon Ω_α , $\boldsymbol{\sigma}^\alpha, \boldsymbol{\varepsilon}^\alpha$ are respectively stresses and strains in Ω_α .

6. DYNAMICAL RESPONSE

If each hexagonal element is considered small enough, dynamical problem can be formulated according to Figure 4 with lumped mass density and dynamical forces, where for the sake of simplicity the influence of rotation is neglected. Suppose the element i is moving while the others in the neighborhood remain stable at some time instant. Then on the element i the following forces act:

In x -direction:

$$\begin{aligned} F_x^{ik} &= k_x^{ik} [u_x^k - u_x^i] + k_{xy}^{ik} [u_y^k - u_y^i] = k_x^{ik} \Delta_x^{ik} + k_{xy}^{ik} \Delta_y^{ik}, \\ F_x^i(t) &= -\rho \frac{d^2}{dt^2} u_x^i(t) \end{aligned} \quad (9)$$

and in y -direction:

$$\begin{aligned} F_y^{ik} &= k_{xy}^{ik} \Delta_x^{ik} + k_y^{ik} \Delta_y^{ik}, \\ F_y^i(t) &= -\rho \frac{d^2}{dt^2} u_y^i(t), \\ F_y^g(t) &= -\rho g \end{aligned} \quad (10)$$

where F_x^{ik} and F_y^{ik} are the forces in springs related to the differences $\{\Delta_x^{ik}, \Delta_y^{ik}\}$ between displacement vector $\{u_x^k, u_y^k\}$ and $\{u_x^i, u_y^i\}$ at the centers of gravity of elements j_k and i by the spring stiffnesses k_x^{ik}, k_y^{ik} , where the neighboring elements are denoted as before $j_k, k = 1, \dots, 6$; F_x^i is the inertia force projected to x -direction, k_y is acting in y -direction, F_y^i is the projection to y -direction, F_y^g is the gravitational force, and ρ is the mass density of the element under consideration.

This simplification is possible only under assumption that the particles are small, i.e. their number is large. Using this facilitation (very similar to classical DEM, as is PFC), also rotations can be involved in the formulation. Because of the clarity of explanation they are omitted and only mentioned in the next paragraphs.

As mentioned above the time steps are expressed in terms of finite differences. At each time step an iteration of new positions of elements is carried out, i.e. the system of pseudo-elliptic equations is solved by iteration. New time step then follows from the values obtained from the latter iteration.

Consider some concrete iteration step in a fixed time. It is obviously necessary to distinguish between iteration of time (this is the primary iteration) and in every time iteration the iteration of position of the nodal points, change of material properties along the interfacial boundaries, assurance of the equilibrium of each particle imbedded in its neighborhood, etc. Then the numerical strategy leads to fixed elements i_1, \dots, i_6 in the neighborhood of element i . The neighboring elements then remain unmovable. The only

displacement at this instant is that of the element i .

$$\begin{aligned} F_n^{ik} &= k_n^{ik} [u_n^k - u_n^i] = k_n^{ik} \Delta_n^{ik}, \\ F_t^{ik} &= k_t^{ik} [u_t^k - u_t^i] = k_t^{ik} \Delta_t^{ik} \end{aligned} \quad (11)$$

where F_n^{ik}, F_t^{ik} are now forces caused by differences between displacement vectors $\{u_n^k, u_t^k\}$ and $\{u_n^i, u_t^i\}$ at the centers of gravity of elements i_k and i , where the neighboring elements are denoted as before $i_k, k = 1, \dots, 6$.

The only problem remains to solve: how to express k_x^{ik}, k_y^{ik} in terms of normal and tangential stiffnesses. Note that the contact forces in Fig. 4 are calculated as:

$$\begin{aligned} N_{ki} &= F_n^{ik} + F_y^g \sin \alpha_{ik}, \\ T_{ki} &= F_t^{ik} + F_y^g \cos \alpha_{ik} \end{aligned} \quad (12)$$

7. SPRING STIFFNESS

The main objective here is to formulate the equations of equilibrium between adjacent elements of each element $i, i = 1, \dots, n$, where n is the number of elements. From this equilibrium it is necessary to determine the displacements of centers of i_k and i , and possibly rotations ϕ_i of each element. Recall that the connection of the adjacent elements is created by the springs with index i (the current disk) and k (j_k are the adjacent elements).

In the sense of (11) the physical equations (Hooke's law applied on the interface) for every couple of adjacent elements are formulated as:

$$\begin{Bmatrix} F_n^{ik} \\ F_t^{ik} \end{Bmatrix} = \begin{bmatrix} k_n^{ik} & 0 \\ 0 & k_t^{ik} \end{bmatrix} \begin{Bmatrix} \Delta_n^{ik} \\ \Delta_t^{ik} \end{Bmatrix} \quad (13)$$

where F_n^{ik}, F_t^{ik} are the normal and tangential forces in the springs on the interface between element i and i_k with spring stiffnesses, and $\Delta_s^{ik} = u_s^i - u_s^k, s = n, t$.

Let the abscissa between elements i_k and i under consideration be deviated from x axis by an angle α_{ik} . Then the transformation of forces to Oxy coordinate system is written by:

$$\begin{Bmatrix} F_x^{ik} \\ F_y^{ik} \end{Bmatrix} = \begin{bmatrix} \cos \alpha_{ik} & -\sin \alpha_{ik} \\ \sin \alpha_{ik} & \cos \alpha_{ik} \end{bmatrix} \begin{Bmatrix} F_n^{ik} \\ F_t^{ik} \end{Bmatrix} = \mathbf{T}_{ik}^T \begin{Bmatrix} F_n^{ik} \\ F_t^{ik} \end{Bmatrix} \quad (14)$$

where \mathbf{T}_{ik} is transformation matrix and superscript T denotes transposition.

Recall a well known fact that \mathbf{T}_{ik} is unitary, it means that $\mathbf{T}_{ik}^{-1} = \mathbf{T}_{ik}^T$. Since the same equations hold for displacements, the following forces-displacements

relation holds valid as:

$$\begin{Bmatrix} F_x^{ik} \\ F_y^{ik} \end{Bmatrix} = \mathbf{T}_{ik}^T \begin{bmatrix} k_n^{ik} & 0 \\ 0 & k_t^{ik} \end{bmatrix} \mathbf{T}_{ik} \begin{Bmatrix} \Delta_x^{ik} \\ \Delta_y^{ik} \end{Bmatrix} = \begin{bmatrix} k_{xx}^{ik} & k_{xy}^{ik} \\ k_{xy}^{ik} & k_{yy}^{ik} \end{bmatrix} \begin{Bmatrix} \Delta_x^{ik} \\ \Delta_y^{ik} \end{Bmatrix} \quad (15)$$

where

$$\begin{aligned} k_x^{ik} &= k_n^{ik} \cos^2 \alpha_{ik} + k_t^{ik} \sin^2 \alpha_{ik}; \\ k_y^{ik} &= k_t^{ik} \cos^2 \alpha_{ik} + k_n^{ik} \sin^2 \alpha_{ik}; \\ k_{xy}^{ik} &= \frac{1}{2} (k_n^{ik} - k_t^{ik}) \sin 2\alpha_{ik} \end{aligned} \quad (16)$$

It remains to express the resultants in the element i , which are in a vector notation denoted as $\{H_i, V_i\}^T$, where H_i is the horizontal component and V_i the vertical one. It simply holds:

$$\begin{Bmatrix} H_i \\ V_i \end{Bmatrix} = \sum_{k=1}^6 \begin{Bmatrix} F_x^{ik} \\ F_y^{ik} \end{Bmatrix} + \begin{Bmatrix} 0 \\ F_g^i \end{Bmatrix} \quad (17)$$

with F_g^i is the gravity at the i -th element. If no rotations were considered, the above formulas would be valid without improvement and the computation may start. Summing the forces in x -direction we get from (9):

$$\begin{aligned} k_x^{ik} \Delta_x^{ik} + k_{xy}^{ik} \Delta_y^{ik} - \rho \frac{d^2}{dt^2} u_x^i(t) &= \\ = k_x^{ik} [u_x^k - u_x^i] + k_{xy}^{ik} [u_y^k - u_y^i] - \rho \frac{d^2}{dt^2} u_x^i(t) &= 0 \end{aligned} \quad (18)$$

and the equilibrium in y -direction follows from (10) as:

$$\begin{aligned} k_{xy}^{ik} \Delta_x^{ik} + k_y^{ik} \Delta_y^{ik} - \rho \frac{d^2}{dt^2} u_y^i(t) &= \\ = k_{xy}^{ik} [u_x^k - u_x^i] + k_y^{ik} [u_y^k - u_y^i] - \rho \frac{d^2}{dt^2} u_y^i(t) - \rho g &= 0 \end{aligned} \quad (19)$$

The latter equations can be unified to the form:

$$\begin{aligned} \frac{d^2 u_x^i}{dt^2} + a_x^i u_x^i + a_{xy}^i u_y^i &= b_x^i, \\ \frac{d^2 u_y^i}{dt^2} + a_y^i u_y^i + a_{yx}^i u_x^i &= b_y^i \end{aligned} \quad (20)$$

In the case of admitted rotations of disks, additional unknown angles describing the rotations of disks have to be introduced. Recall that three DOF (two displacements u', v' and one angle of rotation (ϕ') in 2D are to be sought.

This assertion will be précised in the next text. The solution of latter equation is known as:

$$w(t) = w_0 \frac{\sin \omega \bar{\xi}}{\sin \omega} + w_1 \frac{\sin \omega \xi}{\sin \omega}, \quad \xi = \frac{t - t_0}{h}, \quad (21)$$

$$\omega = h \sqrt{\frac{k_n}{m}}, \quad \bar{\xi} = 1 - \xi$$

where $h = t_1 - t_0$ is the time step, $w_0 = w(t_0)$, $w_1 = w(t_1)$, t_0 is the initial time, t_1 is the time in the next time step. At the middle of the time interval, the value of displacement w and the first derivative by time t are to be determined. It is easy to show that they can be expressed in such a way that both the values and derivatives of the movements are derived as:

$$w_{\frac{1}{2}} = w(\xi = \frac{1}{2}) = \frac{w_0 + w_1}{2 \cos \frac{\omega}{2}}, \quad \frac{d}{dt} w_{\frac{1}{2}} = \frac{\omega(w_1 - w_0)}{2h \sin \frac{\omega}{2}} \quad (22)$$

An important bound estimate follows from equations (21) and (22) on the time step h :

$$h \leq \frac{\pi}{2} \sqrt{\frac{m}{k_n}}.$$

The only troublesome point remains for $k_n \rightarrow 0$. Then linear relation follows from the governing equation and, consequently, the velocity is constant. This is in compliance with the D'Alembert law. The last inequality leads us also to the fact that in the case of large penalty k_n no differences in displacements can be expected due to the inertia forces.

Using the well known approximation formula for second derivative and the above approximate formulas we get:

$$\frac{d^2}{dt^2} w(\xi = \frac{1}{2}) = \frac{1}{4h^2} [w(\xi = 1) - 2w(\xi = \frac{1}{2}) + w(\xi = 0)] \quad (23)$$

which is an explicit formula for calculating $w(\xi = 1)$. Using vector projection to the coordinates system, resulting movement is received. At the moment the center of gravity of the element is then moved assuming the deformed body as rigid.

8. ADDITIONAL DYNAMICAL FORCES INSIDE THE PARTICLE WITH FIXED NEIGHBORHOOD

Additional dynamical forces have to be added to the static formulation. As said above the lumped mass is considered at the center of gravity of each element. The situation is simplified due to this assumption and the calculation of necessary integrals is therefore removed. The volume integrals can also be calculated using a very similar process done by the Eshelby forces. This is no simplification, but possible approach of expressing volume integrals, which are higher order singular. Better approximation is to assume a uniformly distributed inertia forces, which

again leads to unpleasant singular integrals, which cannot be "prefabricated". As mentioned above, our partial aim is to spare the computer consumption and the a priori prepared relations are preferred here. Decoding the equations (16) yields:

$$\sum_{j=1}^6 (K_{ij}^{s11} + k_{11}^{sj} \delta_{ij}) u_1^{sj} + (K_{ij}^{s12} + k_{12}^{sj} \delta_{ij}) u_2^{sj} =$$

$$= k_{11}^{si} u_1^{is} + k_{12}^{si} u_2^{is} + V_1^{si} + Q_1^{si}, \quad (24)$$

$$\sum_{j=1}^6 (K_{ij}^{s21} + k_{21}^{sj} \delta_{ij}) u_1^{sj} + (K_{ij}^{s22} + k_{22}^{sj} \delta_{ij}) u_2^{sj} =$$

$$= k_{21}^{si} u_1^{is} + k_{22}^{si} u_2^{is} + V_2^{si} + Q_2^{si} \quad i = 1, \dots, 6$$

which is a system of 12 equations for 12 unknowns displacements, six in x_1 -direction and six in x_2 -direction. This system is always solved in an iteration step, i.e. the neighboring elements are considered fixed and the value of displacements is taken from the previous step.

9. EXAMPLES

Study on a possible bumps occurrence during long wall mining considering prescribed dislocations is carried out in what follows. Before tackling the concrete problems, some simplifications will be introduced. First the volume weight forces b_i can be neglected, as only a small part of the rock mechanically interacts with the coal seam. The effect of overburden (mostly several hundreds of meters) is simulated as loading along the upper part of the domain describing the whole system rock – coal seam. In this sense the forces \mathbf{V}^{sj} involve only the dynamical effects. There is no aim to delve into details concerning the description of the time development steps, which are based on the finite differences. The formulas for that are exactly the same as those used for the PFC and other distinct element codes. This means that the rotation of particles is suppressed, as this is mostly caused by irregular shape of the particles; cf. (Cundall, 1971), (Cundall and Strack, 1979), (Moreau, 1994). For completeness it is worth noting that if the rotation should be contemplated in the system of equilibrium very similar procedure as introduced in (Procházka, 2004) can be used. The D'Alembert law required and basic relations velocity-movement are based on the simplest stencil in each element s with neighbors $i = 1, \dots, 6$.

The domain describing the problem is a rectangle of 26 m x 9.5 m, the coal seam is 4.75 m high. The regular distribution of hexagons is considered, the internal radius of each hexagon is 0.25 m, the adit has the width 3 m. Number of particles is 1532. Material parameters of the rock mass have the following values (Carmichael, 1989; Bell, 2000): the elastic modulus $E = 50$ GPa, the shear modulus $G = 20$ GPa, the angle of internal friction is 25 degrees, the shear strength $c = 1$ MPa and the

tensile strength $p_n^+ = 100$ kPa. The coal seam is characterized by $E = 5$ GPa, $G = 2$ GPa, the angle of internal friction and the shear strength vary. The load due to the volume weight $\gamma = 25$ kN/m³ is given by the overburden. Depth of the mine is considered as 1000 m. In Figure 5 the set up of hexagonal elements is seen, the shaded part describes the coal seam and the upper part the overburden, which is divided into two parts: the upper part of the overburden simulates the depth of the mine and is characterized by additional loading along the upper boundary of Ω . The lower part of the overburden is described by elastic particles with cohesive boundaries. The boundary conditions of the entire domain are simulated by rollers along the outer boundary, the boundary of the adit has free support, but Eshelby's forces selected according to the current position of the mine face (say, mining shield). They are time dependent and decrease from the extreme values calculated from the virgin state (no opening is created) to the zero value at the time of far enough face from the observed location considered in our examples. The zones of cracked coal seam are simulated by eigenstrains applied inside of the elements, which characterize the inclination of the damage zones. In Figure 6 one predicted dislocation full of gas is shown with its location. The deviation of this dislocation from the horizontal direction is 60° . The toe of the dislocation is 2.5 m from the face of the adit. The shaded particles denote the interface between the coal seam and the overburden. Since the hereditary laws are not considered here, shorter time between the virgin state and the critical state, when the mine face is at a far distance from the observed location, is taken into account. In the following pictures each particular hexagonal element is drawn in the undeformed shape, although they undertake a local deformation (described by movement of the centers of gravity of deformed elements and the deformation of the originally hexagonal shape). The reason is that the accumulation and fictitious overlapping of particles underlines a concentration of stresses. In reality, no overlapping is attained, as the penalty does not allow it.

In Figure 7 the deformation of the coal seam is depicted, belonging to the case of mine face at a far distance from the observed location. A closer view of the picture leads us to the conclusion that the movement of the particles is not only in front of the dislocation but also the particles below the dislocation are disconnected and move slightly. The concentration of elements characterizes stresses along the dislocation in the orientation of the adit.

Figure 8 shows two predisposed dislocations while Figure 10 depicts three predisposed dislocation which are considered in our examples. The movements belonging to the two dislocations are displayed in Figure 9.

The toe of the first dislocation at the lower boundary of the domain is found 2.5 m from the tortuous wall of the mine, the second 5 m from the previous and the third dislocation is next 5 m from the previous dislocation.

Eventually, three dislocations are assumed with the same declination as previous ones and the way of movement, stress concentration and additional cracks are shown in Figure 11. From the pictures it seems to be obvious that the influence of more than one dislocation is not principal in our case of distribution of the damage. The nearer positioned dislocations can affect the possible bumps occurrence. The aim of this paper is only to provide a numerical modeling that can be extended to concrete practical problems. This is why the examples are concentrated on the introduced typical problems. For completeness vectors of movements of particles are seen in Figure 12.

Next a problem of one reverse slope of predicted dislocation full of gas is shown in Figure 13. The inclination of this dislocation from the horizontal direction is 120° .

The following picture, Figure 14, shows the movements at the stage when the mine face is far from the observed cross section. Comparing this with Figure 7 it appears that the cracks are distinct and the bumps have a similar chance of occurrence.

The particles are cast away from the massif but the side face brakes the movement and try to stabilize the opening. The column of the mass on the face, on the other hand, is not stiff enough and probably the coal seam burst will take place. Figure 15 shows two predisposed dislocations while Figure 17 depicts three predisposed dislocation with the inclination 120° . The position of the upper part of the first dislocation is found 2.5 m from the tortuous wall of the mine, the second 5 m from the previous and the third dislocation is next 5 m from the previous dislocation, all measured with respect to the interface between the coal seam and the overburden. Figure 16 introduces the movements of particles, stress concentration and cracks due to two dislocations and Figure 18 describes the same situation in the case of three dislocations.

Figure 19 describes the vectors of movements for three dislocations. Figures 12 and 19 show that in the first case of inclination the mass remains relatively compact, although some cracks appear there. High degree of destruction is observed in the second case of dislocations inside of the coal seam.

It is worth noting that the displacements are small although the overburden is high (1000 m). This is the impact of relative movements caused by Eshelby's forces acting on the side face of mine. In the zone of the predisposed dislocations the movement at the critical point is almost horizontal while on the fringes of the domain describing the problem partly vertical displacements are observed.

In conclusions, the second case of inclination of the dislocations is much dangerous for the bumps occurrence.

Note that the above described approach can be applied to very many cases of predisposed dislocation, even different from 60 or 120 degrees. Then the shape of the elements has to be improved and the regular distribution of the particles is disturbed.

10. CONCLUSIONS

In this paper an application of the free hexagon method, belonging to the discrete elements, to selected problems is presented. Mainly assessment of bumps occurrence in deep mines is studied. Basic relations are formulated showing relatively simple algorithm for preparing computer code, involving natural way of computation of the system of pseudo-linear equations. The time steps are described with an explicit formula, which can be easily used for the problem described by a special loading characterized by the Eshelby forces.

For explication of the theory the influence of inclination of predisposed dislocations in coal seams is presented. Two typical cases are discussed, where the second, the dislocations in which are inclined from horizontal by 120° , are much more dangerous than the case of 60° inclinations. One can esteem that the vertical direction of the dislocations will behave similarly as the first case.

The angles of slopes are obviously selected because of the shape of regular distributed hexagons. As said above the shape of the hexagon in undeformed state can change according to a current geometry of the problem. On the other hand, the vertical dislocations are probably the most complicated geometry, as no chain of hexagons can describe a vertical band with the same width. Then the influence is attained by limit of slightly deviated from vertical line cases. Moreover, the influence of dense dislocations should be studied for certain concrete practical example.

ACKNOWLEDGEMENT

The presented work was supported by the grant of Grant Agency of the Czech Republic no. 103/08/0922 and grant no. 1M0579 of CIDEAS.

REFERENCES

Bell, F.G.: 2000, *Engineering Properties of Soils and Rocks*, Blackwell Publ. house.

Brebbia, C.A., Telles, J.F.C. and Wrobel, L.C.: 1984, *Boundary Element Techniques*. Springer-Verlag, Berlin.

Carmichael, R.S.: 1989, *Practical Handbook of Physical Properties of Rocks*, CRC Press.

Cundall, P.A. and Strack, O.D.L.: 1979, A discrete numerical model for granular assemblies, *Geotechnique*, 47–65.

Cundall, P.A.: 1971, A computer model for simulation progressive large scale movements of blocky rock systems. Symposium of the international society of rock mechanics, 132–150.

Eshelby, J. D.: 1963, The determination of the elastic field of an ellipsoidal inclusion, and related problems, *J. Mech. Phys. Solids*, No. 11, 376–396.

Harami, K.Y. and Brady, B.T.: 1995, A methodology to determine in situ rock mass failure, Internal report of Bureau of Mines. Denver, CO, USA.

Lu, Y.B., Li, Q.M. and Ma, G.W.: 2010, Numerical investigation of the dynamic compressive strength of rocks based on split Hopkinson pressure bar tests, *Int. J. Rock Mech. Min. Sci.*, 47, Issue 5, 829–835.

Ma, G.W., An, X.M. and He, L.: 2010, The numerical manifold method: a review, *Int. J. Numer. Meth.*, Vol. 7, Issue 1, Special Issue: Sp. Iss. SI, 1–32.

Moreau, J.J.: 1994, Some numerical methods in multibody dynamics: Application to granular materials, *Eur. J. Mech. Solids*, 13, No. 4, 93–114.

Procházka, P. and Trčková, J.: 2008, Stress and deformation states in underground structures using coupled modeling. *Acta Geodyn. Geomater.*, 5, No. 4 (152), 361–375.

Procházka, P.P. and Sejnoha, M.: 1995, Development of debond region of lag model, *Computers & Structures*, 55, No. 2, 249–260.

Procházka, P.P. and Vacek, J.: 2002, Comparative Study of Tunnel Face Stability. *Transactions of WIT 37, Fracture and Damage Mechanics VII*, 163–172.

Procházka, P.P.: 2004, Application of discrete element methods to fracture mechanics of rock bursts. *Engng. Fract. Mech.*, No. 71, 601–618.

Wei, X.Y., Zhao, Z.Y. and Gu, J.: 2009, Numerical simulations of rock mass damage induced by underground explosion, *Int. J. Rock Mech. Min. Sci.*, 46, Issue 7, 1206–1213.

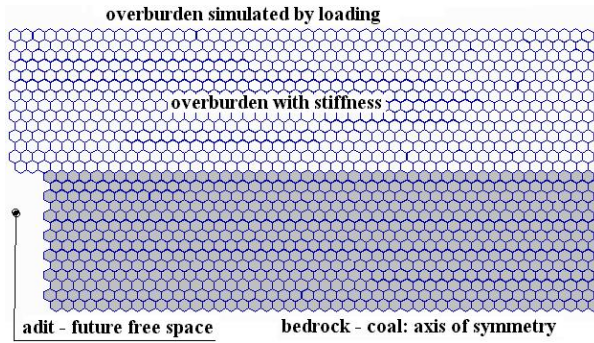


Fig. 5 Set up of the particles.

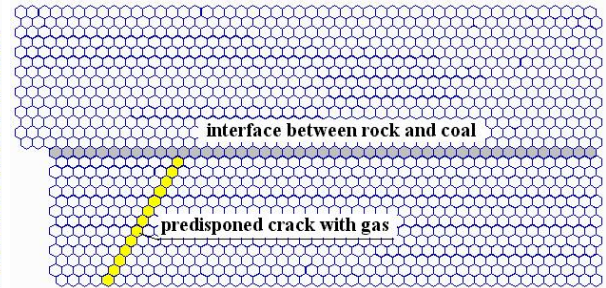


Fig. 6 Location of one predisposed dislocation.

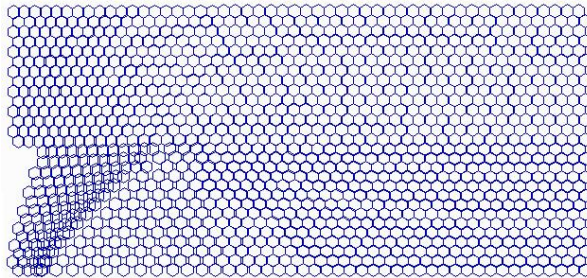


Fig. 7 Movements of the particles, concentration of stresses and additional dislocations, one dislocation.

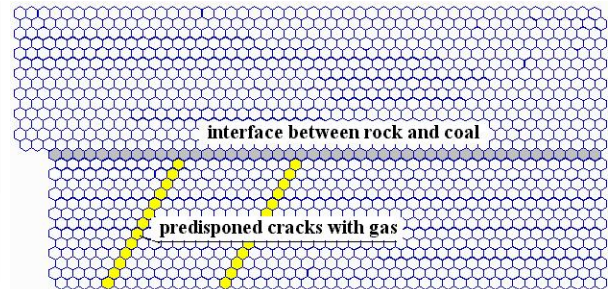


Fig. 8 Location of two predisposed dislocations.

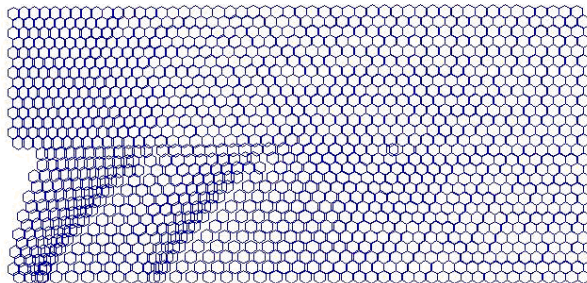


Fig. 9 Way of movements of the particles, concentration of stresses and additional dislocations, two dislocations.

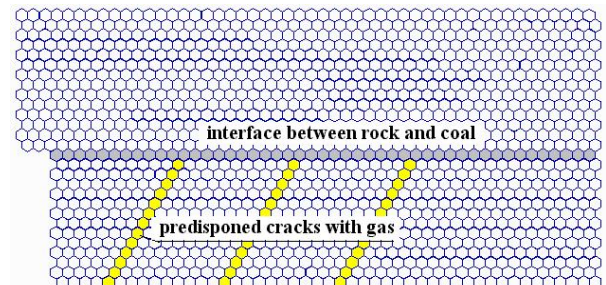


Fig. 10 Location of two predisposed dislocations.

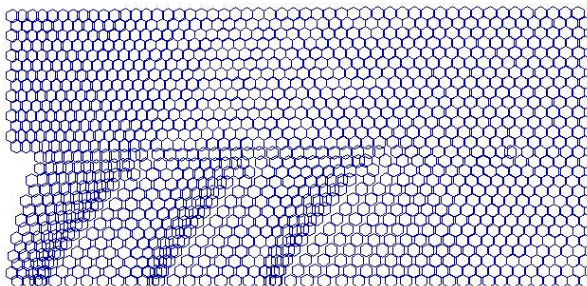


Fig. 11 Way of movements of the particles, concentration of stresses and additional dislocations, three dislocations.

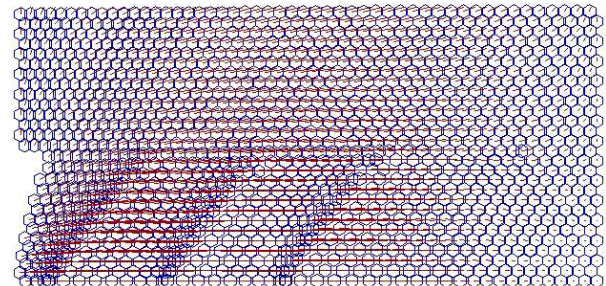


Fig. 12 Vectors of movements of the centers of gravity for three dislocations.

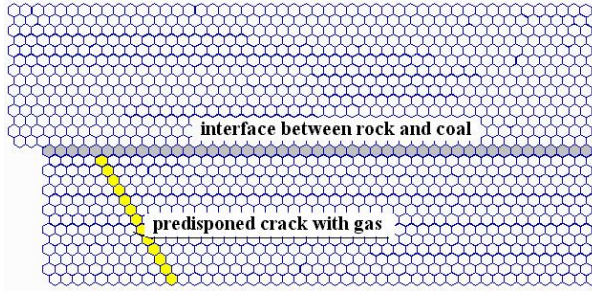


Fig. 13 Location of two predisposed dislocations.

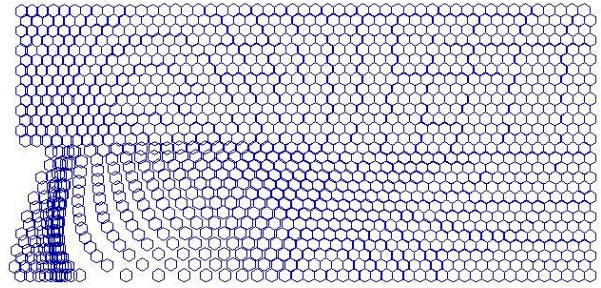


Fig. 14 Movements of the particles, concentration of stresses and additional dislocations, one dislocation.

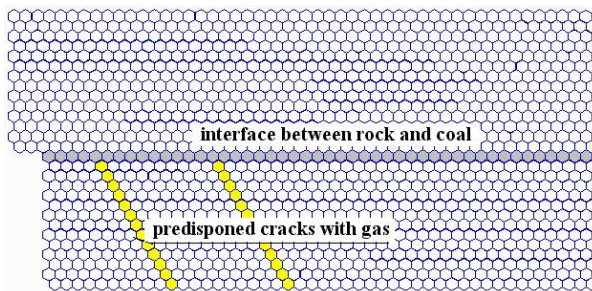


Fig. 15 Location of two predisposed dislocations.

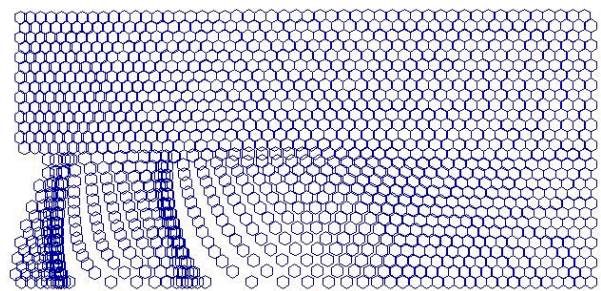


Fig. 16 Movements of the particles, concentration of stresses and additional dislocations, two dislocations.

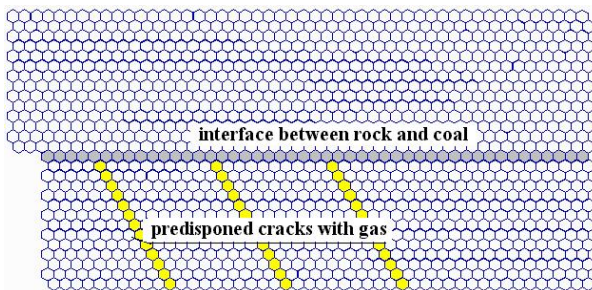


Fig. 17 Location of three predisposed dislocations.

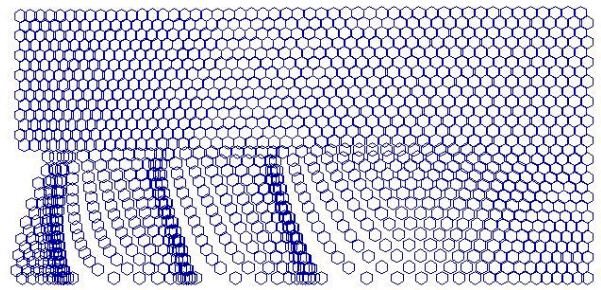


Fig. 18 Way of movements of the particles, concentration of stresses and additional dislocations, three dislocations.

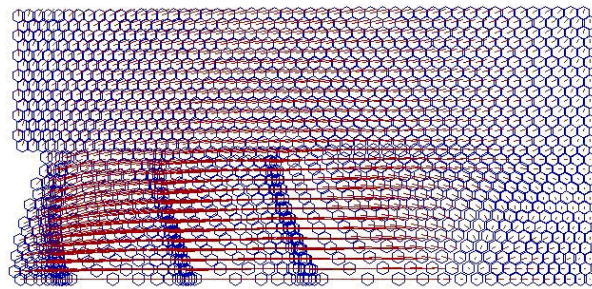


Fig. 19 Vectors of movements of the centers of gravity for three dislocations.